Plant Physiol. (1992) 99, 186–196
0032-0889/92/99/0186/11/$01.00/0

Received for publication July 31, 1991
Accepted December 4, 1991

Radial Turgor and Osmotic Pressure Profiles in Intact and Excised Roots of *Aster tripolium*[1]

Pressure Probe Measurements and Nuclear Magnetic Resonance-Imaging Analysis

Ulrich Zimmermann*, Joachim Rygol, Angelika Balling, Gerd Klöck, Alexander Metzler, and Axel Haase

Lehrstuhl für Biotechnologie, Am Hubland, Biozentrum (U.Z., J.R., A.B., G.K.), and Lehrstuhl für Experimentelle Physik V (Biophysik), Am Hubland (A.M., A.H.), 8700 Würzburg, Germany

ABSTRACT

High-resolution nuclear magnetic resonance images (using very short spin-echo times of 3.8 milliseconds) of cross-sections of excised roots of the halophyte *Aster tripolium* showed radial cell strands separated by air-filled spaces. Radial insertion of the pressure probe (along the cell strands) into roots of intact plants revealed a marked increase of the turgor pressure from the outermost to the sixth cortical layer (from about 0.1–0.6 megapascals). Corresponding measurements of intracellular osmotic pressure in individual cortical cells (by means of a nanoliter osmometer) showed an osmotic pressure gradient of equal magnitude to the turgor pressure. Neither gradient changed significantly when the plants were grown in, or exposed for 1 hour to, media of high salinity. Differences were recorded in the ability of salts and nonelectrolytes to penetrate the apoplast in the root. The reflection coefficients of the cortical cells were approximately 1 for all the solutes tested. Excision of the root from the stem resulted in a collapse of the turgor and osmotic pressure gradients. After about 15 to 30 minutes, the turgor pressure throughout the cortex attained an intermediate (quasistationary) level of about 0.3 megapascals. This value agreed well with the osmotic value deduced from plasmolysis experiments on excised root segments. These and other data provided conclusions about the driving forces for water and solute transport in the roots and about the function of the air-filled radial spaces in water transport. They also showed that excised roots may be artifactual systems.

Much effort has been expended in attempting to reveal the pathways of water transport through roots (3, 7, 8, 10, 11, 14, 18–23). Three parallel, interconnecting pathways from the exterior to the xylem vessels are discussed: the so-called apoplastic or cell-wall pathway (including water-filled intercellulares), the cell-to-cell or transcellular (vacuolar) pathway, and the symplastic pathway via the plasmodesmata. Recent pressure probe work by Steudle and colleagues (20–23) suggested that the apoplastic and the cell-to-cell (but not necessarily the symplastic) pathways may be equally involved in water transport. The conclusion of these authors was derived from comparison of the hydraulic conductivity of the root with that of single root cells, taking the geometry and the number of cell layers into account.

The root hydraulic conductivity was calculated from pressure relaxations induced either hydrostatically or osmotically through excised root segments and by subsequent analysis of the relaxation curves on the basis of the simple phenomenological equations of the thermodynamics of irreversible processes (6, 30). Such a procedure is definitely not free of uncertain assumptions. One problem is the extensibility of the xylem wall. Steudle *et al.* (22, 23) assumed that the xylem vessels are much less extensible than the "root pressure probe" attached to the excised root segments and that the volume change seen was in the apparatus and not in the xylem. However, Balling and Zimmermann (in preparation) showed that the volumetric elastic modulus of the xylem walls of some plants (*e.g.* maize) was very small (comparable to that measured on *Halicystis parvula* [29] and similar to those determined for cell wall tubes of *Characeean* [cited in ref. 30]).

The second problem is the possibility of a disturbance of stationary turgor and osmotic pressure gradients in the tissue when the roots are excised from the plant and water flow through the xylem vessels is stopped. This was suggested by the work of Balling and Zimmermann (1). Evidence for changes in the water parameters in excised tissue was also reported recently by Jones *et al.* (10), who criticized earlier work on excised roots (11) because of the neglect of these changes.

The third problem arises from the large errors involved in the comparison of tissue water permeability with cellular hydraulic conductivity because the actual (and the geometric) water exchange areas are not known.

The fourth problem is due to concentration polarization (unstirred layer) effects (6) if they are neglected in the analysis. This was demonstrated by Büchner and Zimmermann (5) for a model system consisting of a giant algal cell immobilized in a calcium-alginate matrix. These authors showed that the presence of diffusion hindrances and boundary layers in such a porous matrix did not permit any conclusions regarding the water relation parameters of the immobilized cell from osmotically induced pressure relaxation curves.

The fifth uncertainty is the calculation of the water relation parameters of individual root cells, because it is unknown

[1] This work was supported by a grant from the Deutsche Forschungsgemeinschaft (Sonderforschungsbereich 251) to U.Z.

how much flow bypasses the plasmalemma and wall through the plasmodesmata (25).

The interpretative error involved in the analysis of pressure-relaxation curves performed across the total root segment by Steudle and colleagues (20–23) is straightforward if the conflicting data for the L_p[2] values of the whole root segment are considered. For root segments of maize (23), but not of barley (22) or *Phaseolus coccineus* (20), differences of one magnitude in the L_p values were observed when the pressure-relaxation curves across the root were induced osmotically instead of hydrostatically. Interpretation of the differences in the L_p values, in terms of different water pathways through the root segment system considered as a black box, is in contradiction to the second law of thermodynamics (28). The entropy law requires that the water permeability coefficient must be independent of the nature of the driving force, as was experimentally demonstrated for giant algal cells (24) and for leaf cells of *Tradescantia virginiana* (26).

Another problem in the work of Steudle and colleagues is the finding of unusually low values for the reflection coefficients of nonelectrolytes (*e.g.* $\sigma_e = 0.5$ for sucrose) which is in contrast to the literature (7, 8). These authors explained this result in terms of a mosaic membrane structure of the root tissue. However, it is quite likely that the reflection coefficients derived from radial root pressure relaxations reflect the average value of the leaky apoplast ($\sigma_e = 0$) and the impermeable cell membranes ($\sigma_i = 1$) rather than tissue cells with different membrane properties.

To obtain insight into the water transport and pathways through the root, we measured directly the equilibrium turgor pressure (by means of the pressure probe) and the corresponding internal osmotic pressure (by means of a nanoliter osmometer) in individual root cells of intact plants of *Aster tripolium* exposed to different osmotic (and saline) regimens. In separate experiments, we measured the changes in turgor and intracellular osmotic pressure when the roots were excised during the course of the measurements or when the intact root was subject to short-term osmotic pressure regimens. This approach yielded information about the turgor and osmotic pressure profiles in intact and excised roots, an estimation of the reflection coefficients of various solutes for the individual root cells, and information about the osmotic pressure in the local apoplastic space. In addition, these measurements (together with light microscopy and high resolution NMR-imaging investigations) allowed conclusions with regard to the nature of the driving forces for water and solute flows within the root.

MATERIALS AND METHODS

Plant Material

Seeds of *Aster tripolium* (obtained by courtesy of Prof. Westhoff, Leersum/Nijmeger, The Netherlands) were germinated in the greenhouse using square pots containing standard greenhouse soil. After 5 weeks, seedlings were picked and grown in larger pots. During growth, the temperature was 22 to 25°C during the day and 18°C during the night. Simulated daylight (12 h, 400 μmol m^{-2} s^{-1}) was provided by metal halide lamps. The RH of the air was kept at 65%. When the shoots reached a height of about 3 cm and the second foliar leaf had been formed, the roots were washed and placed in aerated culture medium (16) which was replaced every week. After 2 weeks in hydroculture, the plants were transferred into a growth cabinet (12 h/12 h day/night rhythm, light intensity 400 μmol m^{-2} s^{-1}, RH 50/80% during the day/night regimen). Control plants were usually used 5 d after the last medium replacement. The transpiration rate (measured by weighing the total plant) was on average 0.13 mL g^{-1} h^{-1} (fresh weight).

Salt stress was induced by a stepwise increase of the NaCl concentration by 50 mM/d until 300 mM NaCl was reached. One day after establishment of the final salinity, the medium was replaced by fresh medium of equal salinity. Determination of the turgor and internal osmotic pressure of the root cells as well as of the external osmotic pressure was performed in the same medium after 5 d of adaptation by analogy to similar experiments on the roots of *Mesembryanthemum crystallinum* (16).

Cell Dimensions and Morphology

Sections (about 100–200 μm in thickness) were cut with a razor blade at different distances from the root cap (5, 20, and 50 mm). The dimensions of the cells in the various layers were determined as described elsewhere (16). The volume of the rhizodermal cells and of the cortical cells was calculated to be 0.4 to 0.6 and 0.7 to $2.7 \cdot 10^{-4}$ mm^3, respectively.

For demonstration of air-filled intercellular spaces, root segments of about 10 to 20 mm length were placed in the control growth medium, which also contained either 0.05% Trypan blue, 0.1 μg/mL fluorescein, or 5% India ink. After 30 min infiltration of the tissue under vacuum, the root segments were washed three times with growth medium. Cross-sections were cut under oil, covered with immersion oil, and viewed under the (fluorescence) light microscope (Axiophot, Zeiβ, Oberkochen, Germany). Plasmolysis was demonstrated by preincubation of the root segments under vacuum for 30 min in NaCl solutions of increasing osmolarity that contained 20 μg/mL acridine yellow.

Turgor Pressure Measurements

The experimental set-up and the procedure has been described in detail elsewhere (16). Briefly, the taproot of an intact plant (immersed with its complete root system in nutrition medium) was clamped in a Perspex chamber filled with medium of appropriate composition. One of the side roots was mounted in a small channel of 2 mm diameter drilled into the Perspex stage and fixed from the upper side with the clamp. The pressure probe has been described elsewhere (24, 29, 30). Conical or cylindrical microcapillary tips (3–5 μm o.d., 1.5–2.5 μm i.d.) were used. The microcapillary tip and the pressure chamber of the probe were filled with silicone oil.

[2] Abbreviations: L_p, hydraulic conductivity; σ_i, reflection coefficient of internal electrolyte; σ_e, reflection coefficient of external solutes; rf, radiofrequency; T_2, spin-spin relaxation time; T_1, spin-lattice relaxation time; T_E, the time between the excitation of the NMR signal and the detection of the NMR echo.

The radial profile of the turgor pressure through the cortex was measured by insertion of the pressure probe into successive cell layers. Penetration of the next cell was indicated by a stepwise increase in the turgor pressure (see below). The data measured on the rhizodermal cells were discarded because of the large errors caused by the filling of the tip of the microcapillary with cell sap. The boundary between cell sap and oil within the microcapillary tip, which was established about 1 min after insertion into the rhizodermal cells, was kept constant during further penetration by appropriate displacement of the metal rod within the chamber. Because of the dimensions of the tip of the microcapillary, the boundary remained outside the root surface and could, therefore, be accurately monitored under the microscope during the whole penetration procedure. The depth of insertion was determined with a scale in the stereomicroscope and correlated with the cell layers in semithin cross-sections of the side root. After calibration of the insertion depth against the individual cell layers, the turgor pressure (and the osmotic pressure) in cells of a given layer was measured by insertion of the microcapillary tip in one step of appropriate depth into the root tissue.

If not otherwise stated, measurements were performed 50 ± 5 mm away from the root cap. The accuracy of the turgor pressure measurements of cortical cells was ±1 to 3% depending on the cell volume.

The half-time of water exchange between cortical cells in a given layer with the apoplastic space was determined from pressure-relaxation curves. These were induced by injection of pressure pulses of appropriate amplitude into the cells by displacement of the metal rod within the pressure probe. From the half-time of the pressure relaxation, the cellular hydraulic conductivity was calculated according to the method of Zimmermann and Steudle (30). The volumetric elastic modulus of the cells required for the calculation was measured and calculated as usual (16).

Internal Osmotic Pressure

The osmotic pressure of the individual cells was determined using a nanoliter osmometer (Clifton Technical Physics, Hartford, NY). After the cell turgor pressure was determined, a sample of the cell sap was sucked into the microcapillary tip of the pressure probe by generation of an underpressure of 0.02 MPa. This was achieved by appropriate movement of the metal rod of the pressure probe (30). To avoid contamination of the cell sap, the level of the nutrition medium in the root chamber was first decreased below the insertion point of the microcapillary tip by using a vacuum pump (Desaga, Heidelberg, Germany). The remaining residues of solution along the shank of the microcapillary tip were then carefully removed by filter paper before the microcapillary tip was drawn out of the tissue. The cell sap in the microcapillary tip was injected by the metal rod into a droplet of immersion oil placed in the center of the hole of the sample holder under the microscope. The osmotic pressure of the sap was then determined as described elsewhere (13). Control experiments showed that errors arising from evaporation loss were within the limits of accuracy (about 5–10%). As pointed out by Malone *et al.* (13), dilution of the cell sap by uptake of water from the surrounding tissue during the collection procedure can falsify the results under some circumstances. The collection procedure required 8 s at a maximum. Because the half-time of water exchange of the cortical cells was determined to be 14 s (average; see below), dilution errors should not play a significant role. However, the measurements of the osmotic pressure in the very small rhizodermal cells revealed large variations, presumably for the above reasons. Therefore, the data for these cells were not included in the analysis.

Tissue Osmotic Pressure

The average changes of the osmotic pressure of the root tissue (in response to NaCl) were determined in the following way. Roots of intact plants were immersed in the control or solutions of increasing NaCl concentrations for 1 h. Afterward, the roots were carefully washed with distilled water. Part of the side roots were cut, and the 50-mm-long pieces (about 0.1 g fresh weight) were transferred into small glass tubes which were precooled in ice. After liquid nitrogen was added, the tissue was homogenized with a glass rod. Then, the samples were centrifuged for 15 min at 10,000*g*. The supernatant was removed, frozen, and stored for analysis. The osmotic pressure was determined in an aliquot by using the nanoliter osmometer.

Parallel to these experiments, the osmotic pressure of the control or saline media was measured at the end of each experiment.

NMR Microscopy

The theoretical background and the technique has been described in detail elsewhere (9). Briefly, the NMR signal of the hydrogen nuclei in water molecules in living cells and tissues can be spatially localized to create the NMR image of the object. This can be accomplished by the application of a sequence of magnetic field gradients in three directions (9). If these gradients reach values of 100 mT m^{-1}, the spatial resolution of a "water" NMR image can be of the order of 20 μm.

NMR signals can be excited by rf pulses of the characteristic resonance of the nucleus under investigation. The rf pulse transforms "longitudinal" magnetization of the nuclei in the magnetic field into a measurable "transverse" magnetization. This transverse magnetization decays with a time constant, T_2. Fourier transformation of this time-dependent NMR signal gives the NMR spectrum (in the presence of a magnetic field gradient, the NMR projection of the object). The maximum signal is achieved by the application of a 90° pulse. After the rf pulse is applied, the original magnetization recovers by a further relaxation process with the characteristic time constant, T_1.

NMR imaging is performed by the two-dimensional Fourier technique (12). Here, the frequency and phase of the time-dependent NMR signal is changed in a well-defined procedure, yielding a two-dimensional data set, which, after Fourier transformation, results in a two-dimensional NMR cross-sectional image.The NMR-imaging technique used here is a so-called spin-echo technique. The NMR signal intensity, I, in each image element is given by the equation (9, 27):

$$I = k\ N\ (1 - \exp(-T_R/T_1))\ \exp(-T_E/T_2),$$

where N is the proton density, T_R is the repetition time of the NMR experiment, and k is an instrumental constant. Usually, the experiment is performed by using constant values of T_R and T_E. The image contrast and signal intensity is, therefore, dependent on N, T_1, and T_2.

NMR-imaging experiments were performed by means of a 11.75 T vertical magnet of 8.9 cm clear bore (Bruker AMX spectrometer). The magnet contained a Bruker NMR microscope as described elsewhere (27). The experiments were carried out using a 1-mm diameter solenoidal rf coil. For technical reasons, excised side roots bathed in basal medium were investigated. The roots were placed inside a 0.5-mm glass tube. Magnetic gradients of up to 500 mT m^{-1} were applied. A two-dimensional multislice spin-echo-imaging sequence was used to observe the total object without any gap. The repetition time was 3 s, and the echo time was adjusted between 3.8 and 10 ms. The in-plane resolution was 128 × 128 pixels, yielding a spatial resolution of 15 × 15 μm.

The relatively long repetition time and short T_E (minimum 3.8 ms) used here for the NMR image eliminated the influence of both relaxation times, T_1 and T_2. This means that local differences in the brightness of the image are due to differences in the water content. This is an important difference between our measurements and NMR images of plant tissues in the literature (4). In these studies, long T_E values of >20 ms were used. Such images do not show the distribution of water but, rather, the distribution of high water content with long T_2 values. On the other hand, regions with high water content and short T_2 values exhibit low signal intensity when long T_Es are used. This is the case in the presence of proteins and membrane structures.

The use of an extremely short T_E of 3.8 ms or less reduces the signal dependence on T_2. This is a prerequisite to identify the water content as well as the local distributions of mobile water molecules in plant tissues (27).

RESULTS

Radial Cell Strands and Air-Filled Spaces in the Root

The measurement and interpretation of the turgor and intracellular osmotic pressure profiles in the cortex and their adaptation to osmotic changes in the environment require detailed information about the structure of the root.

Figure 1, A and B, shows typical high-resolution NMR microscopy images in the transverse plane of the root of *A. tripolium*. The two images were recorded with different T_Es (10 and 3.8 ms, respectively). Marked variations in the brightness of the proton signals can be seen. The signals from the central water-conducting xylem and phloem vessels were indistinguishable from the surrounding free water. In contrast, the cortex exhibited large regions of low signal intensity with spots of high intensity. At very short T_Es of 3.8 ms, the NMR images showed radial regions of high signal intensity (extending out from the stele to the periphery of the root), separated by regions of low signal intensity (Fig. 1B). Because of the very short T_E, only these areas (volumes) can be attributed to air-filled regions (see above and ref. 27). This assumption was supported by NMR images of root segments preinfiltrated with nutrition medium under vacuum for 30 min (Fig. 1C). In this case, the width of the regions of low signal intensity was very small. The strands of low signal intensity probably reflected dense cell wall material.

The interpretation of the region of low signal intensity in terms of air-filled spaces was also consistent with light microscopy of cross-sections of the roots of *A. tripolium*. Thick cross-sections (>300 μm) had a uniform appearance in light microscopy, in agreement with the report of Brown *et al.* (4). However, thinner cross-sections (about 100 μm) showed that the cortical cells were radially arranged and separated from radial intercellular spaces (Fig. 2A). On average, the cortex consisted of seven to 10 cortical layers. At higher magnifications, a boundary layer with "pits" was seen between the rhizodermis and exodermis (Fig. 2B).

The presence of air in the radial intercellular spaces (as suggested by the NMR images) could be confirmed by infiltrating excised root segments for about 30 min with solutions containing high concentrations of membrane-impermeable dyes (such as Trypan blue and India ink). When infiltration was performed under vacuum, staining of the intercellular spaces could be achieved (data not shown). Otherwise, no uptake of the dye was observed, indicating the presence of air in the intercellular spaces. Convincing evidence was also

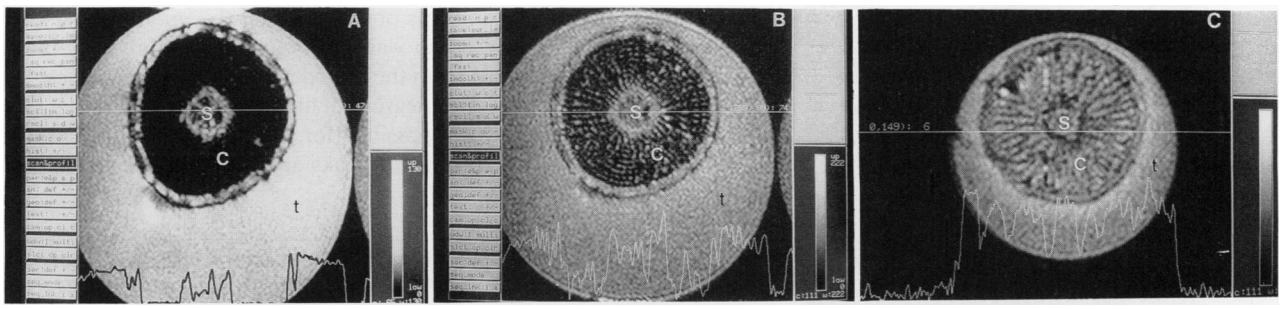

Figure 1. Typical ^1H spin-echo NMR images of cross-sections and signal intensity profiles of excised roots of *A. tripolium*. Slice thickness of projection, 200 μm; field of view, 1 mm diameter; magnetic field strength, 11.5 T; magnetic gradient, 500 mT m^{-1}; matrix, 128 × 128 pixels; resolution, 8 μm. The signal intensity profiles were made along the lines shown in the images. A, T_E 10 ms; B and C, T_Es 3.8 ms; but in C, the root had been preinfiltrated under vacuum with nutrition medium for 30 min. s, Stele; c, cortex; t, tube.

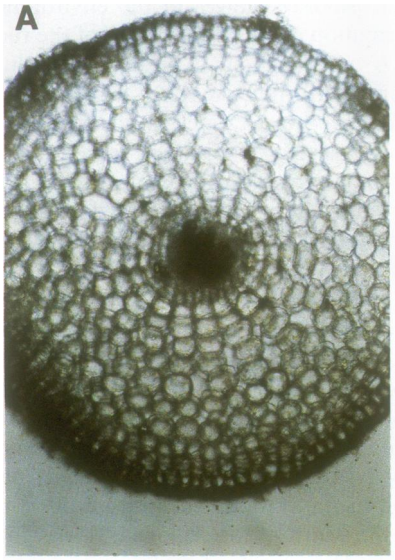

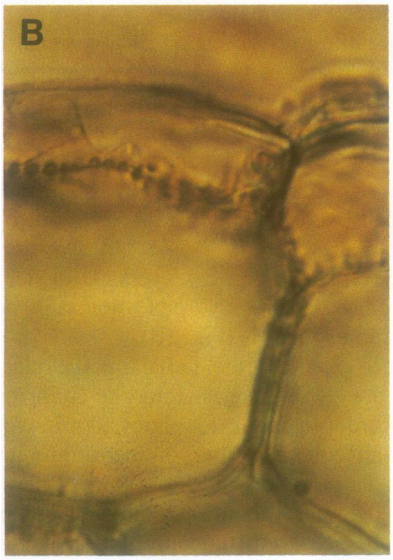

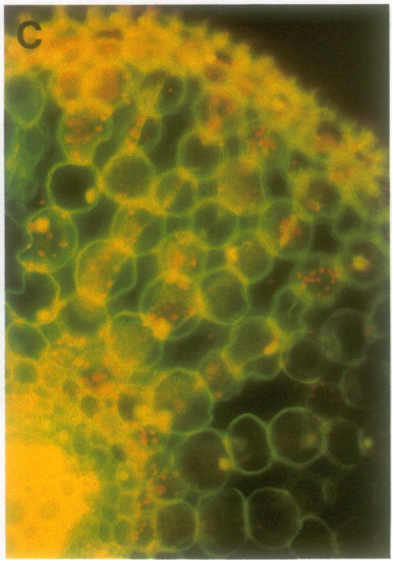

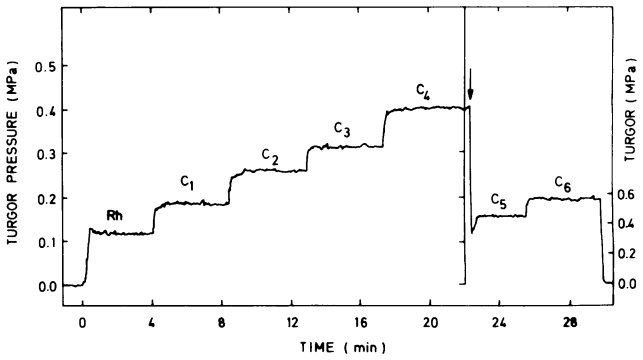

Figure 3. Typical recording of the stepwise changes in turgor pressure during successive insertion of the pressure probe along the radial strands of the cells (Figs. 1 and 2) into the root tissue of intact plants of *A. tripolium*. Measurements were performed 50 mm away from the root cap. Note that the high turgor pressure in the cells of the fifth and sixth cortical layer required a change in the amplification of the recording system (scale on the right).

obtained from plasmolysis experiments on excised root segments with simultaneous staining of the cells with the fluorescent dye, acridine yellow (Fig. 2C). The osmolality was increased stepwise (by addition of appropriate concentrations of NaCl). Plasmolysis of the cells in all cortical layers occurred simultaneously at an osmolality of about 155 mOsmol kg^{-1} (corresponding to an osmotic pressure of about 0.38 MPa) (Fig. 2C). Plasmolysis of cells in discrete cortical layers below this osmolality could not be observed, indicating that the turgor pressure (and the internal osmolality) of the cells was equal throughout the cortex, at least in the excised root segments (see below). The plasmolysis of the cells in the excised root segments also clearly showed that the cortical cells were arranged radially between the stele and periphery of the root (Fig. 2C).

Turgor Pressure Profile and Salinity

Figure 3 shows the turgor pressure profile monitored during radial insertion of the pressure probe into the root tissue of an intact control plant of *A. tripolium* bathed in nutrition medium. Comparable to similar experiments on roots of intact plants of *M. crystallinum* (16), a stepwise increase in turgor pressure was observed when the microcapillary tip of the pressure probe was slowly and discontinuously inserted into the tissue from the rhizodermal to the sixth cortical layer. Turgor pressure measurements beyond this layer (see Fig. 2) were usually not possible (for exceptions, see Fig. 4) because further insertion led to leaks and cracks in the tissue. Meas-

Figure 2. Representative light microscopy cross-sections of excised side roots of *A. tripolium* grown under nonsaline conditions. The sections (about 100 μm thick) were made 50 mm away from the root tip. A, Cross-section of a side root (×40); B, region of the rhizodermis and the exodermis of A viewed at a higher magnification (×400); C, cross-section made after 30 min incubation of the root segment under vacuum in a solution containing acridine yellow and plasmolytic concentrations of NaCl (155 mOsmol kg^{-1}; ×128).

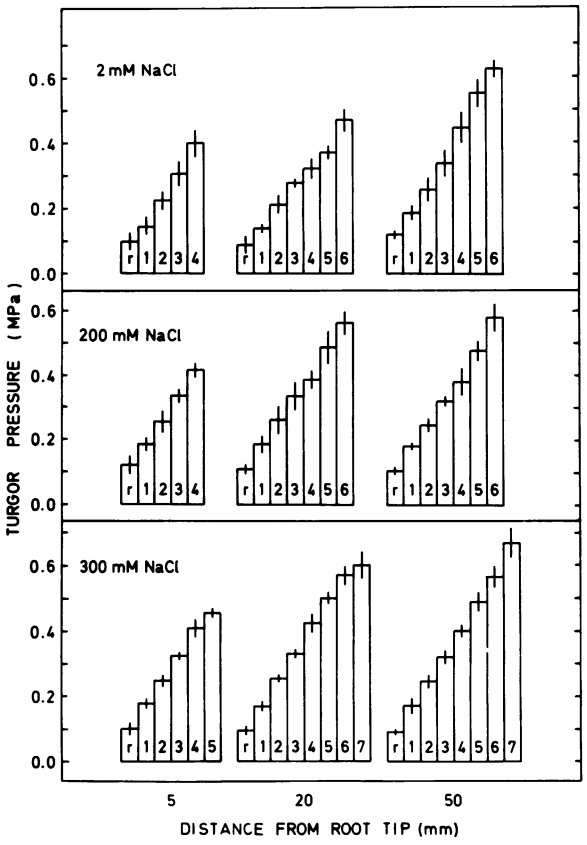

Figure 4. Radial and axial values of the turgor pressure in the rhizodermal (r) and cortical (1–7) cells. Measurements were performed 5, 20, and 50 mm away from the root cap of intact plants of *A. tripolium* grown in nutrition medium (2 mM NaCl) and in the presence of 200 and 300 mM NaCl, respectively, for several days. The data are the means of three to five independent measurements in which a complete pressure profile could be recorded (Fig. 3); bars represent SD. Note that in plants grown in 300 mM NaCl solutions it was also possible to measure the turgor pressure in the seventh cortical layer. From this it is clear that the turgor pressure continued to increase.

urements of the insertion depth and comparison with typical cross-sections as shown in Figure 2 allowed a clear identification of the cell layers.

In many experimental runs, less than seven pressure steps were recorded. The most likely reason for the failure of the measurement of a complete pressure profile was the radial arrangement of the cortical cells. The angle between the microcapillary tip of the pressure probe and the root axis and the orientation of the different cell types to the insertion angle must both be correct to record the complete turgor pressure profile. In cases in which the microcapillary tip penetrated an air-filled space after one or more cell layers, the pressure (measured in relation to atmospheric) decreased to zero. However, it is important to note that in those cases in which the turgor pressure could be recorded in cells from only a few layers the values were identical with those measured in the corresponding cells of a complete run (see below). This finding clearly demonstrated that failure to measure a complete turgor profile was always due to a mismatch between the orientation of the cortical cells and the insertion angle of the pressure probe.

Figure 4 represents the average values of the turgor pressure of the individual cells in the six cortical layers (by pooling the data obtained from complete pressure profile runs). This figure also shows measurements performed 5 and 20 mm away from the root cap. The results demonstrate that radial turgor pressure profiles were not restricted to the 50-mm region. Significant axial cellular turgor pressure gradients did apparently not exist, at least within the experimental accuracy.

It is also interesting to note that, in contrast to the roots of *M. crystallinum* (16), the turgor pressure gradient was nearly maintained when the plants were grown under higher salinity (Fig. 4).

Experiments in which control plants were exposed to short-term salt stress showed that the cortical cells responded to the change in osmotic pressure in the external medium but not to the extent expected from the increase of the external osmotic pressure (Fig. 5). The whole pressure kinetics could not be measured because the microcapillary tip could only be inserted into the cells after replacement of the nutrition media

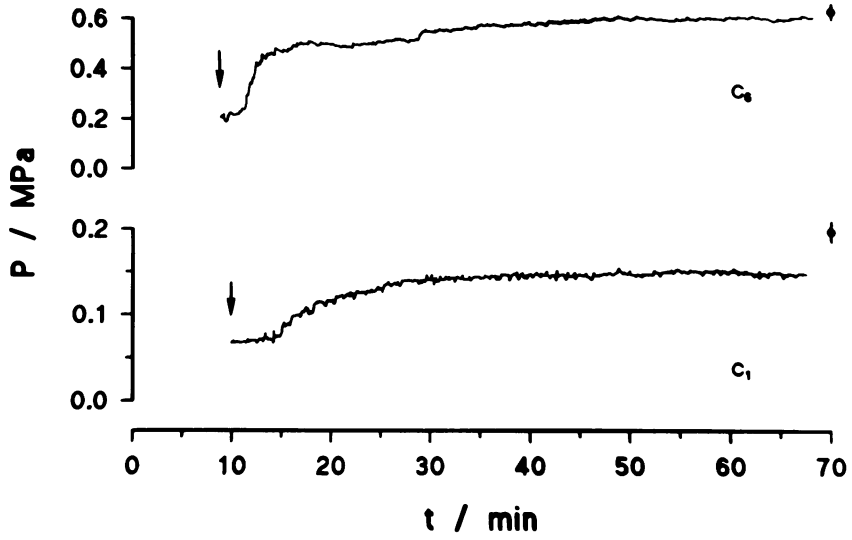

Figure 5. Typical tracings of the turgor pressure recorded with the pressure probe in cells of the first (c_1) and the sixth (c_6) cortical layer of intact plants of *A. tripolium* after replacement of the nutrition medium with 300 mM NaCl solution (t = 0). The pressure probe was inserted 10 min later (arrow). Note that the turgor pressure measured after 10 min was significantly smaller than the average value of the turgor pressure recorded in untreated roots. However, the final value reached after almost 1 h was comparable to that expected from Figure 4 (●).

with 300 mM NaCl solution. However, it is clear from Figure 5 that the turgor pressure in cells of the outermost and the sixth cortical layer was considerably lower after about 10 min of salt exposure than in the control plants. Afterward, the turgor pressure increased again and reached nearly the original value after about 1 h (see also below).

The existence of a stationary radial turgor pressure gradient through the cortical cell layers in the intact plant under normal conditions could also be demonstrated by experiments on control plants in which a few transverse cuts were made through about 20 to 40% of the root diameter at the 50-mm region. Measurements in the cortical cells above the incisions showed no indications that these lesions had affected the radial turgor pressure profile (data not shown). However, below the 50-mm region, the turgor pressure in the cells of all layers decreased very rapidly to low values (<0.05 MPa) without subsequent recovery. The pressure gradients disappeared completely. These results demonstrated that the connection of the cortical cells to the intact xylem vessels (which were most probably damaged by the incisions) appeared to be important for the establishment of turgor pressure gradients.

This could convincingly be demonstrated by experiments (Fig. 6) in which the turgor pressure was recorded in cortical cells of three different layers before and after excision of the side roots. It is clear that the pressure gradient disappeared when the roots were excised (after impalement of the microcapillary tip and recording of a constant turgor pressure value, arrow in Fig. 6). Within about 15 to 30 min, the turgor pressure had almost equilibrated at an intermediate level between the original high turgor pressure value of the sixth

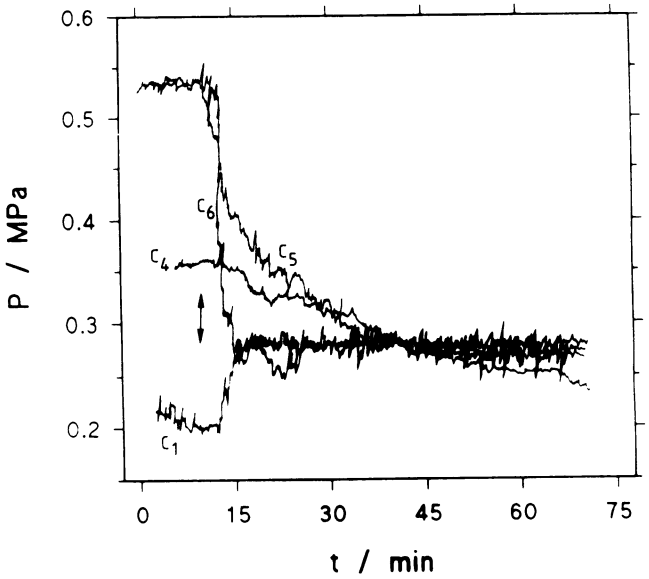

Figure 6. Typical tracings of the turgor pressure in cells of four cortical layers (c_1, c_4, c_5, and c_6) of the root of *A. tripolium* before and after excision (arrow) of the side root from the stem. Note that independently of the original value of the turgor pressure in the individual cells a nearly equal, intermediate turgor pressure value is observed in all cell types after about 15 to 30 min.

and the original low turgor pressure value of the first cortical layer. The new equilibrium turgor pressure of about 0.3 MPa (range between 0.23 and 0.38 MPa, $n = 10$) was comparable with the finding that solutions with an osmotic pressure of about 0.38 MPa were required to induce clear-cut plasmolysis in excised root segments. The observation of a standing radial turgor pressure gradient across the cortex of the intact plant is, therefore, not in contradiction to the finding of equal turgor pressure values in the different cortical layers observed in the plasmolysis experiments (Fig. 2C).

The equilibration time of 15 to 30 min was significantly longer than the average half-time of water exchange of the individual cells.

The half-time of water exchange was determined in separate experiments by injection of volume (pressure) pulses (by means of the pressure probe [30]) into the given cells and by subsequent measurement of the pressure-relaxation curves (data not shown). These experiments yielded an average value of 14.3 ± 3.3 s (mean ± SD; $n = 20$) for the half-time of water exchange. From the pressure-relaxation curves and volumetric elastic modulus of the cortical cells (37 ± 9 MPa, mean ± SD, $n = 14$), the hydraulic conductivity of the cell membranes was calculated to be about $1 \cdot 10^{-8}$ m s^{-1} MPa^{-1}, which is in agreement with other reports (10).

These data suggested that water equilibration between a given cell and its surroundings should occur within 1 min. Therefore, we have to conclude that the establishment of equal turgor pressure values throughout the cortex after excision of the roots must be due to an equalization of the intracellular, osmotically active solutes.

To test this hypothesis, and also to reveal the reasons for the stationary turgor pressure gradient in intact plants, we proceeded to measure the intracellular osmotic pressure in the individual cells under different conditions.

Intracellular Osmotic Pressure Profiles, Reflection Coefficients, Apoplastic Osmotic Pressure, and Salinity

The reproducibility of the measurements of the turgor pressure in the individual cells of the cortex allowed use of this parameter, in addition to the microscopic calibration of the insertion depth, as an indicator of the cell layer. This considerably increased the reliability of the data obtained in the following experiments in which the internal osmotic pressure was determined simultaneously with the turgor pressure (see "Materials and Methods").

Figure 7A shows the mean values for the internal osmotic, and Figure 7B shows the corresponding turgor pressure values of cells in the four cortical layers, c_1, c_2, c_3, and c_6, of intact plants bathed in media of different compositions. The osmotic pressures of cells from the c_4 and c_5 layers were not determined because the procedures for cell sap collection were too time-consuming and difficult.

Comparison of Figure 4 with Figure 7B shows that, under control conditions, the turgor pressure values obtained by averaging single pressure measurements were very similar to those obtained from complete pressure profiles. This excluded the possibility that our method of measuring turgor pressure profiles selected against any tissue structures that did not possess an increasing gradient (see also Figs. 1 and 2).

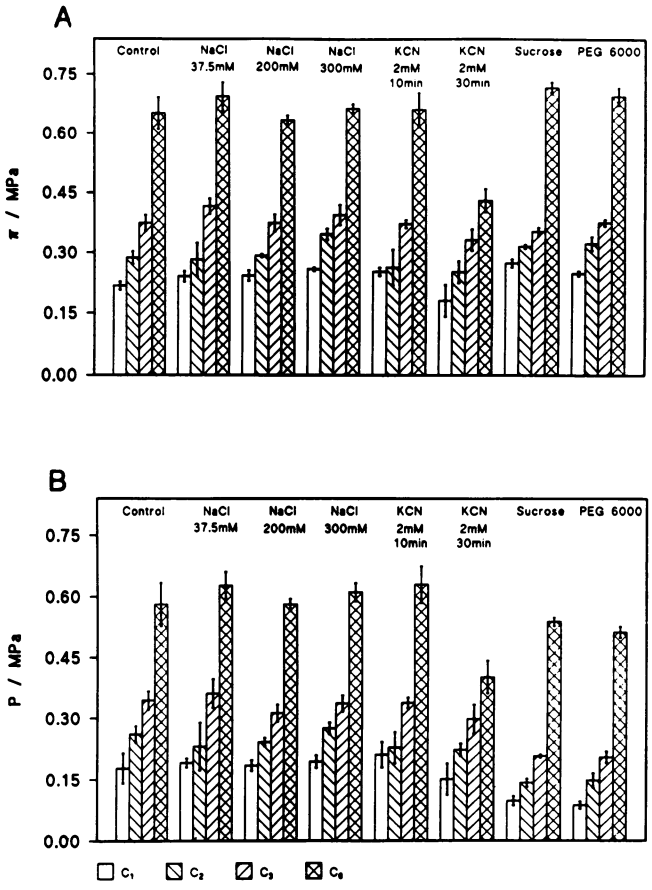

Figure 7. Osmotic (A) and corresponding turgor (B) pressure values recorded in cells of four cortical layers (c_1, c_2, c_3, and c_6) under various short-term osmotic stress conditions. Measurements were performed in the 50-mm region of the root of *A. tripolium* 1 h after addition of the osmoticum (NaCl, sucrose, and PEG) to the nutrition medium. Data are also given for roots that were pretreated with 2 mM KCN for 10 and 30 min, respectively. The data represent means of three to five independent measurements; bars represent SD.

It is also evident from both figures that in the control (but also in the salt-treated plants, see below) the internal osmotic pressure increased continuously from the first to the sixth cortical layer, as in the case of the turgor pressure measurement. In the control plants (final osmotic pressure of the basal medium, $\pi_e = 0.0275$ MPa), the values of the turgor pressure and the corresponding values of the internal osmotic pressure were very similar. It can be easily shown from the raw data that the differences in turgor pressure between cells of different layers were equal to the differences of the corresponding intracellular osmotic pressures. (This is more clearly the case when the turgor and osmotic pressure data of individual cells are compared.) This agreement of the values suggests that the average σ_i of the osmotically active solutes in the cortical cells must be very close to or equal to 1 and, in turn, that the local driving force for water flow between cells of different cortical layers (turgor pressure difference, ΔP, minus intracellular osmotic pressure difference, $\Delta\pi$) was practically zero (or at least very small). Correspondingly, we can conclude that the effective osmotic pressure in the apoplastic space, $\sigma_a \pi_a$, must be very low. With σ_i, $\sigma_a = 1$ and with the assumptions that the apoplastic space was under atmospheric pressure and that water equilibrium between the symplastic and apoplastic space, *i.e.* $\Delta P_{s,a} = \sigma_i\pi_i - \sigma_a\pi_a$, existed (8), the average osmotic pressure in the apoplastic space, π_a, was calculated to be 0.028 MPa, when the data from all cortical cells were pooled. The osmotic pressure in the apoplastic space was apparently equal to the osmotic pressure of the external medium. This conclusion seems to be reasonable and implicitly also justified the assumption of a free equilibration of the ions between the apoplastic and external phases, at least at low electrolyte concentrations.

Analysis of the osmotic pressure of cortical cells in excised roots 1 h after excision showed that the intracellular osmotic pressure in all layers was nearly equal (within the limits of accuracy) and with an average value of 0.35 MPa (range between 0.27 and 0.4 MPa, $n = 10$) also almost identical with the average value of the turgor pressure recorded at the same time (see Fig. 6). The slightly higher value for the intracellular osmotic pressure can easily be explained by a small increase of the osmotic pressure in the apoplastic space due to the redispersal of the intracellular solutes.

The magnitude of the osmotic pressure gradient in roots of intact plants was apparently achieved by active transport. This was demonstrated by poisoning the roots.

Figure 7 presents the turgor and intracellular osmotic pressure values of cortical cells of roots that were bathed in basal medium containing 2 mM KCN. With an incubation time of 10 min, a small, but consistent, decrease of the values of the turgor pressure and internal osmotic pressure for the individual cortical cells could be recorded. With the assumption of σ_i, $\sigma_a = 1$, almost the same value for the apoplastic osmotic pressure is calculated as for the untreated roots. Incubations times of about 30 min resulted in a further, more significant, reduction of the values of both parameters. Despite these lower values, turgor and osmotic pressure gradients could be still recorded (Fig. 7).

In agreement with the salt independence of the radial turgor pressure gradient, no clear-cut salt dependence of the internal osmotic pressure could be detected when the measurements were performed after at least 1 h (Fig. 7). The osmotic pressure of the individual cortical cells was the same in response both to short-term (1 h) and long-term (5 d) exposure of the cells to increasing salt concentration, within experimental accuracy (Figs. 4 and 7A). As in control plants, the term $\Delta P - \Delta\pi$ between the cells of the different layers must, therefore, also be zero at high salinity. This implies that the reflection coefficient of the intracellular osmotically active solutes were still equal to 1. If σ_a is also assumed to be 1, then the osmotic pressure of the apoplastic space in salt-treated plants was only slightly increased (0.056 MPa). If we assume a somewhat lower value for σ_a (about 0.95 MPa), π_a would be comparable to the corresponding value of the control plants. The alternative case that the osmotic pressure in the apoplastic space is high (and in equilibrium with the external medium) and simultaneously $\sigma_a = 0$ could be excluded for two reasons. First, it is extremely unlikely that the reflection coefficients, σ_i, of the internal electrolytes differ markedly from those of the reflection coefficients of the electrolytes of the apoplastic

space, σ_a, although it is well-known that the magnitude of the reflection coefficients depends on the electrolyte concentration (28). Second, in the case of $\sigma_a = 0$ and $\sigma_i = 1$, the intracellular osmotic pressure must increase. This is in contrast to the experimental finding.

In the light of these data, we conclude that salt is excluded from the cortical cells and from the corresponding apoplastic space.

This conclusion could also be supported by measurements of the average tissue osmotic pressure in 50-mm long root segments after a 1-h exposure to increasing NaCl concentrations. The average osmotic pressure increased only by a few milliosmoles per kilogram up to a salt concentration of 200 mM NaCl. At 300 mM NaCl, an increase of about 60 mOsmol kg^{-1} (about 0.15 MPa) was observed, which is equivalent to an uptake of about 30 mM NaCl into the tissue. This amount is relatively small, particularly if part of the salt is transported to other parts of the roots (*e.g.* to the xylem vessels [17]). This assumption is consistent with the measurement of the turgor pressure in the individual root cells of intact plants after replacement of the nutrition medium by 300 mM NaCl (Fig. 5). The instantaneous decrease in turgor pressure was also much less than expected from the external osmolarity. The subsequent recovery of the turgor pressure shows that the electrolyte must be removed from the apoplastic space in the cortex to other regions of the root which were not investigated.

Osmotic Response of the Cortical Cells after Addition of Nonelectrolytes

In the following set of experiments, we measured the turgor and internal osmotic pressure in the individual cells of the cortical layers of control plants after short-term osmotic stress induced by nonelectrolytes. This was achieved by addition of 75 mOsmol NaCl, sucrose, or PEG (mol wt 6000) to the basal medium. Measurements were made after 1 h incubation. In contrast to NaCl, addition of the nonelectrolytes resulted in a stationary decrease of the turgor pressure and in a corresponding increase of the internal osmotic pressure in all cortical cells as expected for an ideal osmometer (Fig. 7). If we assume that σ_i of the intracellular electrolytes is still equal to 1 and that the solutes in the apoplastic space (electrolytes and the given nonelectrolyte) have a reflection coefficient of $\sigma_a = 1$, the average osmotic pressure of the apoplastic space, π_a, is calculated to be about 0.175 MPa. This value agrees very well with the osmotic pressure of the external medium. Thus, we can conclude that the apoplastic space was in osmotic equilibrium with the external medium.

DISCUSSION

Measurements of turgor pressure and internal osmotic pressure on the cellular level were performed on intact and excised roots of *A. tripolium*. Most of the studies were restricted to the region 50 mm away from the root cap where water usually enters the tissue most rapidly (3). However, the few measurements of the turgor pressure profile in the 5- and 20-mm regions of *A. tripolium* suggested that the water relations and osmotic regulation phenomena there were comparable to those in the 50-mm region.

As in the case of *M. crystallinum* (16), the existence of radial turgor and osmotic pressure gradients could be demonstrated. The turgor and intracellular osmotic pressure increased continuously between the first and the sixth cortical layers. In contrast, other authors (11, 15, 22, 23) reported that turgor pressure was constant across the cellular layers of the roots of wheat and maize. Only in the stele was an elevated turgor pressure recorded (15).

The presence or absence of radial turgor and osmotic pressure profiles in the roots can, *a priori*, be explained by the assumption of plant-specific and/or age-dependent differences between halophytes and glycophytes. In our studies, we used halophytes that were about 2 months old, whereas the groups of Tomos and Steudle worked with roots of glycophytes that were 5 to 13 d old. It is quite conceivable that during cell growth and enlargement radial turgor and intracellular osmotic pressure profiles cannot develop because of the high demand for solute and water uptake (but see also below).

However, in light of the experiments reported here (Fig. 6), the possibility that pressure gradients originally present in the excised root segments (as used *e.g.* by Steudle and colleagues) had collapsed cannot be excluded. Indirect evidence for this was already given by Tomos and colleagues (10, 11), although these authors did not recognize the possible reason for their observation. Jones *et al.* (10) found that the value of the root hydraulic conductivity depended on the time after excision and explained this in terms of different water pathways. In addition, they reported a dependence of the root hydraulic conductivity on the root length when measured 90 min after excision. We showed for *A. tripolium* that the turgor (and osmotic) pressure gradients disappeared within about 15 to 30 min after excision of the side roots. The turgor pressure and the intracellular osmotic pressure assumed constant and nearly equal values throughout the cells of the cortical layers. However, results obtained on osmoregulation phenomena in single cells (30) suggest that this state may only be maintained temporarily in the excised roots. Because of the compartmentation and the intricate coupling of passive and active flows and forces in the root, the hydrostatic and osmotic driving forces within the symplast cannot be considered in isolation from other transport processes (such as active transport). Therefore, prolonged radial and axial effects in the root segments are to be expected before a true osmotic equilibrium between the external medium and the apoplastic and symplastic spaces in the whole tissue is reached. Data obtained from measurements of excised roots must be interpreted with caution.

The collapse of the pressure gradients after excision of the root (together with the other experimental data) permits two conclusions. First, the decrease of the turgor pressure in the cells of the innermost cortical layers and the corresponding increase of the turgor pressure in the cells of the outermost cortical layer (after excision of the root) toward a quasistationary, intermediate level represents (in addition to the arguments given above) unequivocal evidence for the existence of such gradients in the *in vivo* system. Second, the solute flow into the xylem vessels must be induced by solvent drag, and the corresponding water flow must be driven by the difference between the xylem pressure (tension) and atmos-

phere. These conclusions are straightforward if we consider the pressure data and the morphological appearance of the root.

P and π were equal ($\sigma_i = 1$) for the individual cells in adjacent cortical layers before excision of the root in a saline or nonsaline environment. The driving force for water flow through the cortical cells is, therefore, (nearly) zero. Furthermore, the osmotic pressure estimated for the apoplastic space was either equal (under nonsaline conditions) to or considerably less (under saline conditions) than the osmotic pressure of the external medium (calculated according to the van't Hoff equation). This suggests that under saline conditions water is osmotically driven from the apoplastic space to the external medium. Under this condition, net water flow through the apoplastic space of the tissue can only be understood as being due to the difference between the xylem pressure and atmosphere. This pressure difference must exceed the osmotic pressure difference between the apoplastic space and the external medium (*i.e.* about 1.5 MPa in 300 mM NaCl solution). In light of recent results of direct pressure (tension) measurements in xylem vessels of intact higher plants (1, 2), such pressure differences seem to be unlikely. The xylem pressure values were between atmospheric and zero or just on the negative side of zero.

However, for water transport, the difference in the effective osmotic pressures, $\sigma \cdot \Delta\pi$, is the responsible osmotic driving force. If we assume the extreme case that the reflection coefficients of the electrolytes in the external media are zero, the effective osmotic pressure must correspondingly also be zero. Thus, an osmotic driven component of the water flow directed from the apoplastic space to the outside does not exist. In this case, pressure values in the xylem somewhat below atmospheric (or slightly negative) would be sufficient to drive water from the external medium to the xylem vessels (1, 2), provided that water flows through this pathway (see below).

At first glance, the assumption that $\sigma_e = 0$ for the external electrolytes is difficult to understand because this means that electrolytes should freely enter the root tissue. This is not the case as shown by the data of the osmotic pressure of the bulk tissue as well as by the only temporary decrease of turgor pressure in the cortical cells of an intact plant in response to a sudden, large increase of the salt concentration (Fig. 5). These findings showed that the root tissue was apparently protected against a high salt concentration. Consistently, analysis of the turgor and osmotic pressure data suggested that the osmotic pressure in the apoplastic space increased only slightly when the salt was increased in the external medium.

This discrepancy can be resolved if we take into account the "pit"-containing boundary between the rhizodermis and the exodermis. It is quite likely that water and ions can only enter the tissue through these small pits. It can be envisaged that the diffusion through the pits may be rather limited, probably also because of the charged walls of the pits and the connected apoplastic space. In addition, the volume of the apoplastic space is very small because of the presence of the large radially oriented air-filled spaces. These radial "rays" of air-filled spaces extending from the stele to the exterior could be clearly identified by high-resolution NMR microscopy. At the short T_E of 3.8 ms, the NMR signals reflect the spatial water content (27). A signal dependence on the T_2 can be definitely excluded when this T_E is used (see above)[3].

It is clear that the pit-containing boundary (together with the air-filled spaces) must provide a large resistance to solute (and water) flow (19). In this case, the uptake of electrolytes into the tissue is relatively low, in agreement with the experimental results, even if $\sigma_e = 0$ for the external electrolytes.

If the roots are excised, the flow/force pattern must change. If the pressure difference between the xylem vessels and the atmosphere remains unaltered (1, 2), the collapse of the turgor and osmotic pressure gradients in the cortical layers cannot be primarily induced by changes in the water flow. Therefore, the very first response of the system after excision must be a concentration-driven solute flow from the innermost cortical layer (6, 30) to the external medium. This leads to the conclusion that this diffusional flow was balanced in the intact system by a solvent drag-driven component, J_s', of the solute flow directed into the xylem ($J_s' = [1 - \sigma]\, \bar{c}_s\, J_v$, where c_s is the average concentration of the solute between the xylem vessels and the cortex). The water flow, J_v (which has the dimension of a velocity), is the only parameter that disappeared immediately after the roots were excised. Therefore, an outwardly directed solute flow is initiated along the concentration gradient.

If this interpretation of the data is correct, we have to assume that water flow must pass through at least some of the cellular layers between xylem and rhizodermis. It is also clear that an osmotic pressure gradient in the cortex can only be established if the solute flow induced by solvent drag exceeds a critical value.

The absence of pressure gradients in the roots of intact wheat plants (15) may, therefore, be due to a nonsufficient flow velocity through the xylem vessels. Pritchard *et al.* (15) used plants (see above) and conditions in which the transpiration rate was very small. Although flow and transpiration rate are not necessarily closely coupled (2), it is conceivable that in these plants the water flow (velocity) in the xylem vessels was too low to create a solvent drag-driven solute flow.

The active component of the solute flow (also directed toward the xylem) should not be affected by excision of the root (at least not immediately). Therefore, it is unlikely that this component has a major influence on the outward directed diffusional component of the solute flow. The data presented here suggest that in the intact roots active transport processes were mainly required for the maintenance of the magnitude of the osmotic balance in the individual cells. Continuous accumulation of the osmotically active substances within the cells is required because of the stationary loss of solutes by solvent drag transport to the xylem. These conclusions are supported by the KCN experiments. After pretreatment of

[3] The presence of radial regions of low intensity were also reported by Brown *et al.* (4) for roots of *Pelargonium hortorum* and interpreted in terms of radial cell layers through which water is not transported equally. However, in contrast to our work, these authors used T_Es of 20 ms (or more). At such long T_Es, the T_1 and T_2 relaxation times contribute to the signal intensity. Therefore, it is very likely that the interpretation of the NMR images performed on *P. hortorum* by Brown *et al.* (4) was not correct.

the intact roots with KCN, the turgor pressure and the intracellular osmotic pressure values decreased proportionally in all layers. However, gradients of both parameters between the inner- and outermost cortical layers still existed. This is expected if the osmotic balance in the individual cells is achieved mainly by the oppositely directed solvent drag and diffusional components of the solute flow. Both components are proportional to the average concentration of the osmotically active solutes in the cells (see above).

However, the role of active transport processes must also be seen in the reversal of passive solute leakage through the plasma membrane into the apoplastic space. It is clear that the dimensions of the apoplastic space around the cells must correlate with the activity of the pumps to maintain the radial pressure gradients. The plants apparently achieve this requirement by separation of the cell strands by the air-filled spaces.

Finally, the different responses to salt stress, on the one hand, and nonelectrolyte, on the other, mean that the uptake of nonelectrolytes (such as sucrose and PEG) into the apoplastic space has one of two extreme alternative characteristics. It must be either completely free or else prevented (presumably by the pit-containing boundary). In both cases, a stationary decrease of the turgor pressure values in the cortical cells is expected because the system behaves like an ideal osmometer. This follows from the agreement of the calculated value of the osmotic pressure in the apoplastic space with that of the external medium (*i.e.* 0.175 MPa).

It should also be mentioned, that a consistent view of the different responses of the root tissue cells after the addition of electrolytes and nonelectrolytes was only achieved when the reflection coefficients of the cortical cells for the various solutes were assumed to be (close to) 1. The finding of a reflection coefficient of 1 for nonelectrolytes is in agreement with Fiscus (7) and other authors (14) but in contrast to Steudle and coworkers (23). There is no necessity and no plausible reason to assume (significantly) lower σ_e values than 1 for sucrose or PEG 6000.

ACKNOWLEDGMENTS

We are very grateful to Dr. W.M. Arnold for reading and discussing the manuscript. We thank Prof. Dr. O.L. Lange for the opportunity to conduct part of the work in the Institute of Botany, University of Würzburg.

LITERATURE CITED

1. **Balling A, Zimmermann U** (1990) Comparative measurements of the xylem pressure of *Nicotiana* plants by means of the pressure bomb and pressure probe. Planta **182:** 325–338
2. **Benkert R, Balling A, Zimmermann U** (1991) Direct measurements of the pressure and flow in the xylem vessels of *Nicotiana tabacum* and their dependence on flow resistance and transpiration rate. Bot Acta **104:** 47–52
3. **Boyer JS** (1985) Water transport. Annu Rev Plant Physiol **36:** 473–516
4. **Brown JM, Johnson GA, Kramer PJ** (1986) *In vivo* magnetic resonance microscopy of changing water content in *Pelargonium hortorum* roots. Plant Physiol **82:** 1158–1160
5. **Büchner K-H, Zimmermann U** (1982) Water relations of immobilized giant algal cells. Planta **154:** 318–325
6. **Dainty J** (1963) Water relations of plant cells. Adv Bot Res **1:** 279–326
7. **Fiscus EL** (1975) The interaction between osmotic- and pressure-induced water flow in plant roots. Plant Physiol **55:** 917–922
8. **Fiscus EL** (1977) Determination of hydraulic and osmotic properties of soybean root systems. Plant Physiol **59:** 1013–1020
9. **Gadian DG** (1982) Nuclear Magnetic Resonance and Its Application to Living Systems. Clarendon Press, Oxford, United Kingdom
10. **Jones H, Leigh RA, Wyn Jones RG, Tomos AD** (1988) The integration of whole-root and cellular hydraulic conductivities in cereal roots. Planta **174:** 1–7
11. **Jones H, Tomos AD, Leigh RA, Wyn Jones RG** (1983) Water-relation parameters of epidermal and cortical cells in the primary root of *Triticum aestivum* L. Planta **158:** 230–236
12. **Kumar A, Welt D, Ernst RR** (1975) NMR-Fourier Zeugmatography. J Magn Reson **18:** 69–83
13. **Malone M, Leigh RA, Tomos AD** (1989) Extraction and analysis of sap from individual wheat leaf cells: the effect of sampling speed on the osmotic pressure of extracted sap. Plant Cell Environ **12:** 919–926
14. **Miller DM** (1985) Studies of root function of *Zea mays*. III. Xylem sap composition at maximum root pressure provides evidence of active transport into the xylem and a measurement of the reflection coefficient of the root. Plant Physiol **77:** 162–167
15. **Pritchard J, Williams G, Wyn Jones RG, Tomos AD** (1989) Radial turgor pressure profiles in growing and mature zones of wheat roots: a modification of the pressure probe. J Exp Bot **40:** 567–571
16. **Rygol J, Zimmermann U** (1990) Radial and axial turgor pressure measurements in individual root cells of *Mesembryanthemum crystallinum* grown under various saline conditions. Plant Cell Environ **13:** 15–26
17. **Shennan C, Hunt R, Macrobbie EAC** (1987) Salt tolerance in *Aster tripolium* L. II. Ionic regulation. Plant Cell Environ **10:** 67–74
18. **Spanswick RM** (1976) Symplastic transport in tissues. *In* U Lüttge, MG Pitman, eds, Encyclopedia of Plant Physiology, New Series, Vol II: Transport in Plants, II Part B: Tissues and Organs. Springer-Verlag, New York, pp 35–56
19. **Stelzer R, Läuchli A** (1977) Salt and flooding tolerance of *Puccinellia peisonis*. II. Structural differentiation of the root in relation to function. Z Pflanzenphysiol **84:** 95–108
20. **Steudle E, Brinckmann E** (1989) The osmometer model of the root: water and solute relations of roots of *Phaseolus coccineus*. Bot Acta **102:** 85–95
21. **Steudle E, Frensch J** (1989) Osmotic responses of maize roots. Water and solute relations. Planta **177:** 281–295
22. **Steudle E, Jeschke WD** (1983) Water transport in barley roots. Planta **158:** 237–248
23. **Steudle E, Oren R, Schulze ED** (1987) Water transport in maize roots. Measurement of hydraulic conductivity, solute permeability, and of reflexion coefficients of excised roots using the root pressure probe. Plant Physiol **84:** 1220–1232
24. **Steudle E, Zimmermann U** (1971) Hydraulische Leitfähigkeit von *Valonia utricularis*. Z Naturforsch **26b/12:** 1302–1311
25. **Tomos AD** (1988) Cellular water relations of plants. *In* F Franks, ed, Water Science Reviews 3. Cambridge University Press, Cambridge, United Kingdom, pp 186–277
26. **Tyerman SD, Steudle E** (1982) Comparison between osmotic and hydrostatic water flows in a higher plant cell: determination of hydraulic conductivities and reflection coefficients in isolated epidermis of *Tradescantia virginiana*. Austr J Plant Physiol **9:** 461–479
27. **Walter L, Balling A, Zimmermann U, Haase A, Kuhn W** (1989) Nuclear-magnetic-resonance imaging of leaves of *Mesembryanthemum crystallinum* L. plants grown at high salinity. Planta **178:** 524–530
28. **Woermann D** (1976) Mass transport across membranes. *In* CR Stocking, U Heber, eds, Encyclopedia of Plant Physiology, New Series, Vol III: Transport in Plants, III: Intracellular Interactions and Transport Processes. Springer-Verlag, New York, pp 419–464
29. **Zimmermann U, Hüsken D** (1980) Turgor pressure and cell volume relaxation in *Halicystis parvula*. J Membr Biol **56:** 55–64
30. **Zimmermann U, Steudle E** (1978) Physical aspects of water relations of plant cells. Adv Bot Res **6:** 45–117